Climatic Change (2026) 179:149
https://doi.org/10.1007/s10584-026-04235-z

Increasing risk of 2022-like droughts in Europe under climate change: evidence from Large Ensembles using flow analogs

Burak Bulut[1] · **Salvatore Pascale**[2] · **Davide Faranda**[3]

Received: 8 October 2025 / Accepted: 11 June 2026

Abstract
The 2022 European drought was exceptional in spatial extent, intensity, and duration, with severe impacts on society and ecosystems. Its primary dynamical driver was a persistent anticyclonic anomaly over the eastern North Atlantic and western Europe. While anthropogenic climate change (ACC) is known to intensify droughts thermodynamically by enhancing evaporation, its impact on atmospheric circulation patterns remains uncertain due to strong internal variability. Using seven Single Model Initial-condition Large Ensembles (SMILEs) and a flow analog approach, we assess the influence of ACC on both dynamical and thermodynamical aspects of the 2022 drought. Specifically, we examine changes in the spatial structure and frequency of circulation analogs, as well as the conditional probability of drought occurrence. Our findings indicate that ACC did not significantly alter the pattern or frequency of the circulation drivers linked to the 2022 drought, even under higher levels of global warming. However, it markedly increases the likelihood of severe drought given such circulation patterns, resulting in broader spatial extent, greater intensity, and reduced intra-analog variability. These results suggest a shift in drought causation under global warming, with thermodynamic factors increasingly dominating over dynamical drivers.

Keywords Droughts · Anthropogenic climate change · Flow analogs · Large ensembles · Extreme event attribution

✉ Salvatore Pascale
salvatore.pascale@unibo.it

[1] UK Centre for Ecology and Hydrology, Wallingford OX10 8BB, UK

[2] Department of Physics and Astronomy, University of Bologna, via Irnerio 46, 40126 Bologna, Italy

[3] Laboratoire des Sciences du Climat et de l'Environnement, UMR 8212 CEA-CNRS-UVSQ, University Paris-Saclay, IPSL, l'Orme des Merisiers, Bat 714, Gif-sur-Yvette 91191, France

Published online: 24 June 2026

1 Introduction

In 2022, Europe experienced a drought of exceptional intensity and duration (Toreti et al. 2022a; Garrido-Perez et al. 2024; Pascale and Ragone 2025). The prolonged precipitation deficit, combined with higher-than-average temperatures (Bevacqua et al. 2024), resulted in a hydrological drought of widespread societal and environmental impacts in the latter half of that year (Baruth et al. 2022), especially in northern Italy (Clifford 2022; Navarra 2022; Montanari et al. 2023), France, Spain, Portugal and the Netherlands (Toreti et al. 2022a). The significant societal costs of the 2022 drought quickly drew the attention of the scientific community and the media to the role of Anthropogenic Climate Change (ACC) in creating the conditions for this extreme event.

Understanding how ACC is currently affecting these events and how it will affect them in a future warmer climate is a pressing concern for water managers and decision-makers tasked with addressing future water crises (Wendt et al. 2021, Kreibich, H. et al., 2022; Teutschbein et al. 2023). As for all other meteorological and climatic extreme events, evaluating the effects of ACC on extreme drought events requires assessing changes in large-scale circulation drivers - the dynamic contribution - as well as changes driven by temperature increase - the thermodynamic contribution (NAS 2016; Shepherd 2016, 2019; Yiou et al. 2017). These two contributions can reinforce each other when large-scale circulation anomalies (e.g., persistent anticyclones) reduce precipitation while higher temperatures enhance evapotranspiration, jointly intensifying soil moisture deficits and drought severity. Human-caused global warming is already exacerbating soil moisture droughts by enhancing atmospheric water vapor demand, evapotranspiration, and hence soil drying (Lehner et al. 2017; García-Herrera et al. 2019; Allan et al. 2021; Massari et al. 2022; Gebrechorkos et al. 2025). Recent studies (Faranda et al. 2023; Schumacher et al. 2024) confirm that the 2022 drought too was exacerbated by ACC. Specifically, Bevacqua et al. (2024) find that ACC contributed to over 30% of the drought intensity and its spatial extent through enhanced evapotranspiration, with a substantial fraction of the contribution mediated by warming-driven soil drying occurred before year 2022.

While the thermodynamic contribution of ACC to recent extreme droughts is understood, it remains difficult to attribute changes in atmospheric circulation dynamics directly to ACC (Shepherd 2014; Seneviratne et al. 2021). Indeed, there are few studies in which the effect of ACC on atmospheric circulation in single meteorological drought events has been identified (Harrington et al. 2016; Odoulami et al. 2023). Recent research discusses a positive trend in springtime and summertime 500 hPa geopotential heights over Europe in the last forty years (Christidis and Stott 2015), correlating that with recent European drying (Bakke et al. 2023). However, it remains challenging to discern the exact role of ACC on such large scale dynamical changes conditions in specific events, given the substantial role played by internal atmospheric variability and by the limitations global climate models in reproducing the atmospheric dynamics (Shepherd 2014; Lehner and Deser 2023; Shaw et al. 2024; Doane-Solomon et al. 2025).

A weather regime analysis by Garrido-Perez et al. (2024) shows that the 2022 drought was due to an unusual frequency of high-pressure systems over western Europe and to a significant shift in blocking activity towards the south, with a consequent poleward displacement of the North Atlantic eddy-driven jet. In terms of atmospheric low-frequency variability, the dynamic driver of the 2022 drought was a record-breaking positive anoma-

lies in geopotential height over the eastern North Atlantic and western Europe (Faranda et al. 2022; Pascale and Ragone 2025). The persistence of the above-mentioned anticyclonic anomaly has also been related to the sequential occurrences of specific phases of modes of atmospheric low-frequency variability, i.e., the North Atlantic Oscillation (NAO), the East Atlantic Pattern (EA), the Scandinavian Pattern (SCAND), and the East Atlantic/Western Russian Pattern (EAWR). Pascale and Ragone (2025) show that a strong EA+ and EAWR- in late spring-summer 2021 followed in winter-spring 2021–2022 by a strong SCAND- and a NAO+ and then by a EA+ EAWR- in summer 2022 contributed to maintaining the above-mentioned positive pressure and geopotential height anomalies

Using the century-long 20CR reanalysis (Compo et al. 2011) along with a flow analog approach (Yiou and Nogaj 2004; Jézéquel et al. 2018; Vautard et al. 2021), Faranda et al. (2023) investigated the exceptionality of the persisting anticyclonic anomaly over the Atlantic and Western Europe which drove the 2022 drought. They identified such anticyclonic pattern as the 9-month averaged 500 hPa geopotential height anomaly (December 2021 - August 2022) and then searched for atmospheric flow analogs in the 9-month low-pass filtered data. By comparing the periods 1836–1915 to 1942–2021, they showed that the more recent analogs of the 2022 circulation anomalies were associated with higher near-surface temperatures and geopotential heights, and lower values of the Standardized Precipitation-Evapotranspiration Index (Vicente-Serrano et al. 2010). These findings, while indicating an exacerbation of the event by ACC, also show that, in terms of meteorological drivers, there were no decadal trends in the frequency of occurrence of this analogs over the observed period, that is, no evidence that atmospheric low-frequency anomalies as those observed in association with the 2022 drought have become more frequent in the recent decades. A major limitation of Faranda et al. (2023) is that it relies only on observations (i.e., reanalysis data), which makes it impossible to totally rule out the internal variability signals, which, at the decadal and multidecadal scales, can be comparable in the near-mid term (see, e.g., Kay et al. 2015; Deser et al. 2020). Furthermore, for certain variables (e.g., dynamical variables, Staten et al. 2018; Shaw et al. 2024), the forced signal may not have emerged yet from the internal variability noise.

In this study, we expand the results of Faranda et al. (2023) about the 2022 Euro-Mediterranean drought and apply their methods to a suite of 7 Single Model Initial-condition Large Ensembles (SMILEs, e.g., Kay et al. 2015; Deser et al. 2020; Maher et al. 2021) available in the CMIP6 archive (Eyring et al. 2016). SMILEs provide thousands of years of data, facilitating robust statistical estimates of hydroclimatic extremes (Van der Wiel et al. 2019) - contingent upon their accurate representation of climate variability (Simpson et al. 2025). Additionally, they facilitate the quantification of the range of internal variability and the identification of the forced signals associated with ACC. In Europe, precipitation features significant internal variability across timescales ranging from subseasonal to decadal, due to atmospheric low-frequency modes (e.g., NAO, Barnston and Livezey 1987; Hurrell 1995; Keeley et al. 2012; Gastineau and Frankignoul 2015; Woollings et al. 2015) as well as the remote effects of sea surface temperature anomalies (e.g.,the Atlantic Multidecadal Variability Knight et al. 2005; Sutton and Hodson 2005; Kucharski et al. 2006; Brönnimann 2007; Zampieri et al. 2017). Consequently, utilizing a large ensemble of climate projections is a powerful method for separating internal natural variability from forced signals at decadal timescales. Employing more than one SMILE allows for the assessment of model structural uncertainty (Deser 2020). SMILEs proved to be very useful to study the contribu-

tion of ACC to exceptional multi-year droughts, as, for example, the 2015–2018 "Day Zero" drought in Cape Town, South Africa (Otto et al. 2018; Sousa et al. 2018; Wolski 2018; Pascale et al. 2020; Odoulami et al. 2023), the 2015–2019 Central American drought (Pascale et al. 2021; Anderson et al. 2023), and the 2018–19 drought in the river Rhine basin (Van der Wiel et al. 2022) as well as to understand how these events may look like in the future at higher levels of global warming.

By analyzing different SMILEs across past, present, and future climates, we aim to understand how droughts like the 2022 event in Europe evolve when the same large-scale atmospheric circulation patterns occur, helping us isolate the role of ACC. Specifically, in this study we are addressing the three following points: How does ACC affect the spatial structure of atmospheric circulation analogs over time? Does the frequency of occurrence of circulation analogs shift under the influence of ACC? To what extent does ACC modify the likelihood of drought conditions associated with specific circulation analogs?

The paper is structured as follows: in Sect. 2, we describe the data and the methods used to identify low-frequency flow analogs which drove the 2022 drought event; in Sect. 3, we present the main results of this study, which are then critically discussed in Sect. 4 and summarised in Sect. 5.

2 Data and methods

2.1 Drought and circulation variables

The Standardized Precipitation Evapotranspiration Index (SPEI) evaluates drought severity by integrating precipitation and potential evapotranspiration (Vicente-Serrano et al. 2010). SPEI extends the Standardized Precipitation Index (SPI) (McKee et al. 1993) by including atmospheric water demand, estimated here via the simplified Thornthwaite method based solely on temperature, due to limited GCM data availability. Given the multi-year 2022 drought (Pascale and Ragone 2025), we use the 12-month SPEI (SPEI12) to track long-term droughts, a standard for hydrological drought assessment (Spinoni et al. 2013, 2015). Atmospheric circulation patterns are identified using monthly 500 hPa geopotential height (Z500) fields and their corresponding anomalies (see Sect. 2.2 for details on the computation of Z500 anomalies), alongside monthly precipitation and near-surface temperature, to analyze SPEI variations during droughts.

2.2 Observations

The SPEI dataset, obtained at a $0.5° \times 0.5°$ horizontal resolution from the Global SPEI database (SPEIbase v2.10, Beguería et al. 2014), is derived from monthly potential evapotranspiration and precipitation data provided by the CRU TS v4.08 dataset (Harris et al. 2020). It covers the period from January 1901 to December 2023.

To identify anomalous atmospheric circulation linked to the drought over the North Atlantic-European sector, we employ monthly ERA5 reanalysis (Hersbach et al. 2020) from 1940 to 2022. The 500 hPa geopotential height (Z500) data are detrended via a 3rd-order polynomial and deseasonalized by subtracting long-term monthly means (1940–2022). A 12-month backward moving average aligns with the SPEI12 timescale (Kingston et al.

2015). The circulation analog search (Sect. 2.4) targets the 12-month averaged Z500 anomaly for August 2022, when the drought reached its maximum extent and severity (Bevacqua et al. 2024; Pascale and Ragone 2025).

2.3 Single model initial-condition large ensembles

We use seven SMILEs derived from CMIP6 GCMs with varying resolutions: ACCESS-ESM1-5, CanESM5, GISS-E2-1-G, IPSL-CM6A-LR, MIROC6, MPI-ESM1-2-LR, and UKESM1-0-LL. These models were selected because they provide at least 10 ensemble members for both the historical (1850–2014) and future (2015–2100) periods. Models with fewer members were excluded due to their limited ability to sample internal climate variability (Milinski et al. 2020). For future projections, we consider two Shared Socioeconomic Pathways: SSP3-7.0 (high emissions) and SSP5-8.5 (very high emissions) (Riahi et al. 2017). To facilitate comparison, all model outputs were resampled to the spatial resolution of MPI-ESM1-2-LR ($1.875° \times 1.875°$). Details on the GCMs are provided in Table S1 (see Supplementary Information). We use monthly means of 500 hPa geopotential height, precipitation, and near-surface temperature.

Historical (1850–2014) and future projections (2015–2100) of precipitation, temperature and Z500 were combined to obtain a dataset spanning from 1850 to 2100. As with ERA5, SMILE Z500 anomalies were calculated by detrending, deseasonalizing, and smoothing the data using a 12-month backward moving average. All processing was performed separately for each ensemble member. For the Pre-Industrial period (1851–1900), the mean was removed, while the post-1900 period was detrended at each grid cell using a third-order polynomial fit. Monthly seasonality was then removed by subtracting the long-term monthly means computed over 1851–2100 from the detrended data, so that each monthly anomaly represents the deviation from its corresponding calendar-month mean over the full period. The resulting anomalies were then smoothed using the 12-month moving average

2.4 Flow analog analysis

The target field for the flow analog search is the 12-month average Z500 anomaly in August 2022 (Fig. 1b) relative to the September 2021-August 2022 mean Z500 (Fig. 1a). Here and in the rest of the paper, we will refer to low-frequency atmospheric states that are very similar to this target circulation anomaly as the "flow analogs". While this method cannot fully capture the complex dynamics of droughts, previous studies (Faranda et al. 2023; Pascale and Ragone 2025) clearly show that multi-year droughts are associated with persistent anticyclonic circulation patterns, which lead to sustained positive pressure and Z500 anomalies over the entire duration of the event.

The search is conducted within each ensemble member of every SMILE, considering both the historical period and future projections under two SSP scenarios (SSP3-7.0 and SSP5-8.5). The flow analog method allows for a decomposition (e.g., Shepherd 2016) of the joint probability of experiencing a European drought $\mathcal{D}$ (Fig. 1f) and a given circulation state $\mathcal{C}$ (Fig. 1b) as observed in 2022. Specifically, this joint probability can be expressed as $P(\mathcal{D},\mathcal{C}) = P(\mathcal{C})P(\mathcal{D}|\mathcal{C})$, where $P(\mathcal{D}|\mathcal{C})$ represents the probability of the 2022 drought conditional on the circulation state $\mathcal{C}$, and $P(\mathcal{C})$ is the probability of that circulation state. Thus, this approach enables us to investigate the following three objectives:

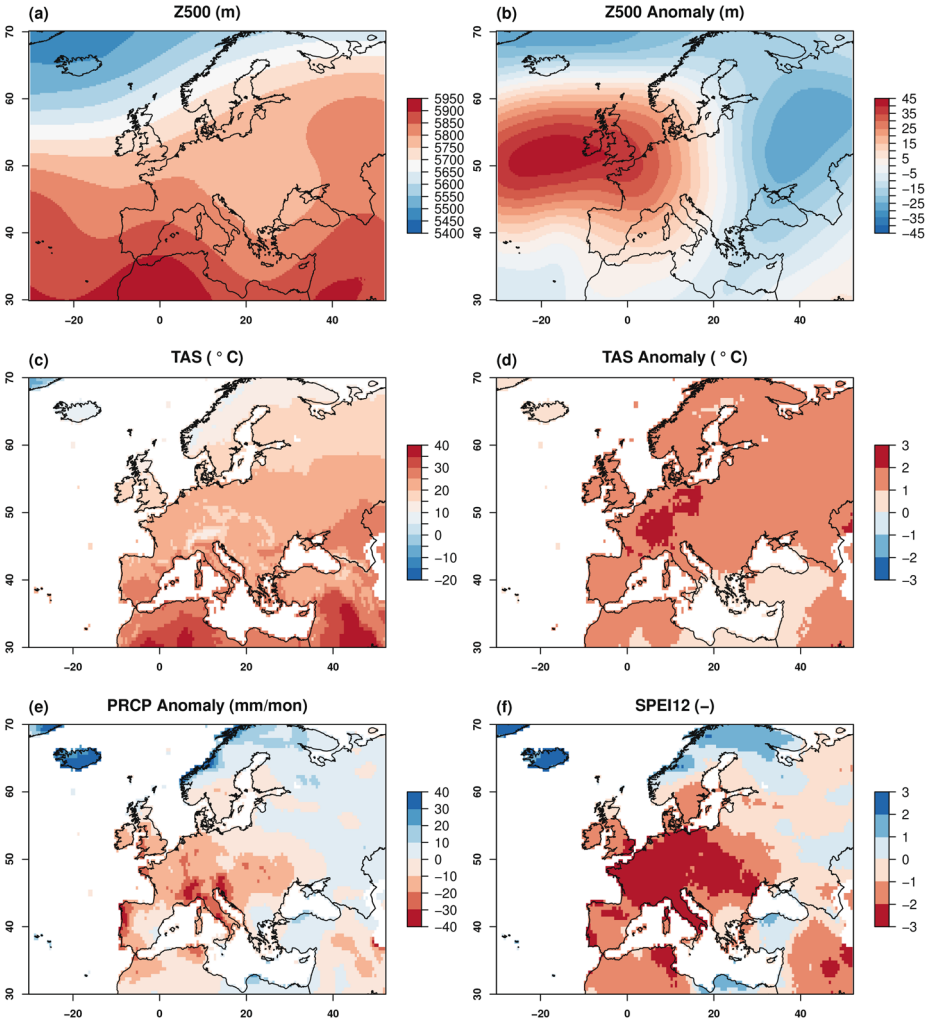

Fig. 1 Main climatological features of the 2022 drought event: (**a**) Z500, (**b**) Z500 anomaly, (**c**) Near surface temperature (2 m), (**d**) Near surface temperature anomaly, (**e**) Precipitation anomaly, (**f**) SPEI12. Time means are are taken over the period September 2021-August 2022 in order to be consistent with the calculation of SPEI12. Anomalies are computed relative to the baseline periods 1940–2022 for ERA5 data (panel b) and 1901–2022 for CRU and SPEIbase data (panels d and e)

1. to evaluate if the spatial pattern of circulation analogs $\mathcal{C}$ changes in time under the effect of ACC;
2. to evaluate if the frequency with which these circulation analogs happen changes in time under the effect of ACC (i.e., $P(\mathcal{C})$);
3. to evaluate if, during analogs, drought conditions are more or less prone to develop under the effect of ACC (i.e., $P(\mathcal{D}|\mathcal{C})$).

2.4.1 Evaluating changes in flow analog patterns

To evaluate the spatial patterns of the analogs, we define five 50-year periods (Supplementary Fig. 1) during which flow analogs are sought: Pre-Industrial (PI, 1851–1900), Far Past (FP, 1901–1950), Near Past (NP, 1951–2000), Near Term (NT, 2001–2050), and Far Future (FF, 2051–2100). The use of 50-year windows is motivated by the requirement to capture a sufficient number of events comparable to the 2022 multi-year drought, thereby ensuring the robustness and statistical significance of the analysis. The PI period serves as a baseline representing internal climate variability without the influence of anthropogenic climate change (ACC), effectively acting as a *counterfactual* climate (NAS 2016).

We place particular emphasis on the NT period (2001–2050), which includes the time frame of the 2022 drought and is therefore relevant for contextualizing this event within contemporary climate conditions. We note that the climate during this period is non-stationary; thus, the NT window should not be interpreted as a fixed "present climate", but rather as a near-term warming context within which the 2022 drought evolved. The FF period (2051–2100) represents climatic conditions associated with approximately +3–4 K of global warming relative to the PI baseline, a level that may be reached by the end of the century without rapid and substantial mitigation efforts (e.g., Allan et al. 2021).

Following the extensive literature on circulation analogues (e.g., Yiou 2014; Jézéquel et al. 2018; Yiou et al. 2021; Faranda et al. 2023), we identify flow analogues by minimizing the Euclidean distance between reanalysis-based and GCM-based Z500 anomaly fields. While alternative distance metrics can be used which accounts for the spatial covariance structure of the fields (see discussion in Yiou 2014), they are substantially more computationally expensive than the Euclidean distance, which is therefore preferred.

For each period, SMILE, and ensemble member, the five best analogs—those with the smallest distance values—are selected. Consequently, each ensemble member of a GCM contributes 25 analogs in total (5 analogs per period).

For each GCM, the average of all selected analog maps (i.e., 5 maps per ensemble member multiplied by the number of ensemble members) is computed. For instance, the IPSL model's Z500 anomaly composite for the FF period is generated by averaging 55 analog maps (11 ensemble members for SSP3-7.0). Analogous averaging is applied to temperature, precipitation, and drought maps associated with the analog months to facilitate a comprehensive analysis.

At the multimodel level, for each SSP scenario and selected period, analogs from all GCMs are combined by averaging to produce multimodel mean maps—for example, averaging 1,185 analog maps for the SSP3-7.0 scenario for a given period. A schematic overview of this methodology is presented in Supplementary Fig. 1.

2.4.2 Evaluating changes in flow analog frequency

To assess the frequency of analog occurrences, we define, for each SMILE, a fixed Euclidean distance threshold corresponding to the 0.05 quantile of all distances computed over the full 1851–2100 period across all ensemble members. This threshold is then used to identify analogs and their timing throughout the entire record (1851–2100), for each SMILE and each ensemble member, and to determine the time window (e.g., PI, FP) in which they occur. This approach allows us to quantify changes in flow analog frequency as the climate

evolves, for example by comparing the number of analogs occurring in 2051–2100 with those in 1851–1900.

3 Results

3.1 Impact of ACC on flow analog patterns

Figure 1a and b illustrate the 12-month mean Z500 and Z500 anomalies for August 2022. These fields reflect the prevailing large-scale atmospheric circulation that contributed to the maximum drought extent and intensity observed. Specifically, a persistent high-pressure ridge over western Europe is characterized by a significant positive Z500 anomaly in this region and the northern Atlantic (Faranda et al. 2023). Near-surface temperature (Fig. 1c) was substantially above average (Fig. 1d) in the 12-month period September 2021-August 2022, contributing, along with precipitation deficits (Fig. 1e) to negative SPEI12 values over most of Europe (Fig. 1f).

The 12-month mean Z500 (Fig. 1a) is notably exceptional, with values generally exceeding those found in simulated analogs across various periods (Fig. 2a). The anomaly analogs for Z500 simulated by SMILEs are illustrated in Fig. 2b, showing a notable similarity to those observed in 2022 (Fig. 1b). This highlights the capability of GCMs to accurately capture the 12-month circulation anomaly.

The differences in Z500 (Fig. 2d, g, j, m) during FP, NT, and FF compared to values during the PI period allow us to assess the extent to which the low-frequency flow analogs that contributed to the 2022 drought are being significantly impacted by ACC in terms of shape, position, and magnitude. Models consistently indicate a non-uniform increase of Z500 with warming in the analogs, demonstrating that Z500 gradually and consistently rises from FP to FF. This increase is more pronounced in eastern Europe than in western Europe, with the largest increments observed over northwestern Europe and northern Africa, and the smallest increments over the North Atlantic (Fig. 2j-m). Such pattern is consistently similar to what observed under the SSP5-8.5 scenario too (Supplementary Fig. 2).

Unlike the full Z500 field, it is less clear how ACC will affect the shape and position of the Z500 anomalies in the analogs (Fig. 2b, e, h, k, n). When examining the multimodel multimember ensemble mean differences between NT, FF, and PI, a dipolar structure emerges first in NT and then persists and strengthens in FF (Fig. 2l, o). This dipole is characterized by positive anomalies over Eastern Europe and negative anomalies over Western Europe. The signals observed in NT and FF are consistent with those in SSP5-8.5 (Supplementary Fig. 2). This suggests that this pattern might not just be noise, but rather a significant part of the forced signal in the Z500 anomaly for this low-frequency flow analog. By examining the individual SMILEs involved in this study, we find that three out of four GCMs - CanESM, MIROC, and MPI - exhibit similar responses, featuring the same dipolar structure as the multimodel ensemble (Fig. 2o, and Supplementary Figs. 3, 4, 5). In contrast, the remaining models (ACCESS, GISS, IPSL, and UKMO) show quite different responses compared to both the multimodel ensemble mean and each other (Fig. 2o, Supplementary Figs. 6, 7, 8, 9). Similar differences in Z500 anomalies and patterns across GCMs are consistently observed in the single model figures for SSP5-8.5 as well (not shown).

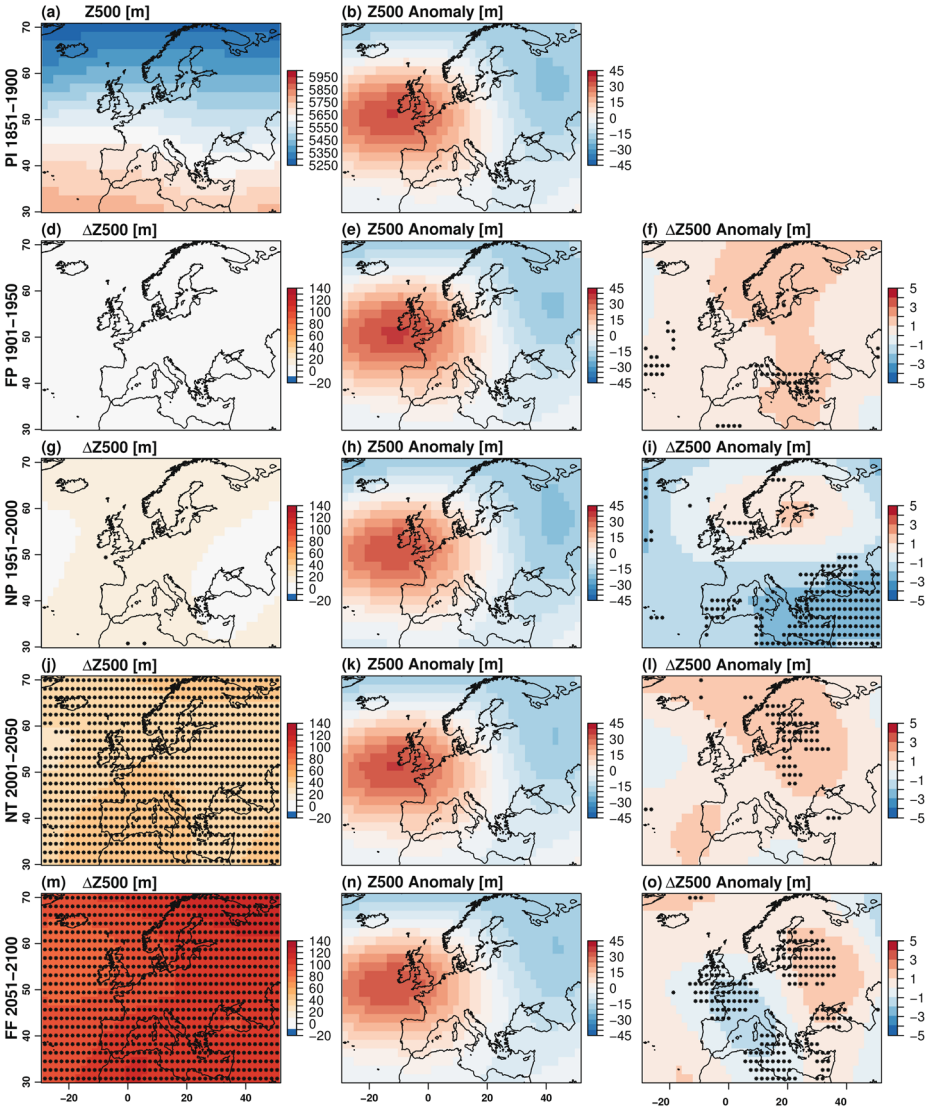

Fig. 2 Flow analogs from SMILEs for historical and future periods (2015–2100 from SSP3-7.0). (**a**) Mean Z500 and (**b**) Z500 anomalies during PI flow analogs. (**d**) FP-PI differences in Z500 associated with flow analogs. (**e**) Z500 anomalies during FP flow analogs. (**f**) FP–PI differences in Z500 anomalies. (g–i), (j–l), and (m–o) as in (d–f), but for the NP, NT, and FF periods, respectively. Stippling indicates inter-model agreement (at least 5 GCMs showing statistically significant change). For each GCM, differences from PI are computed for the selected period using $N = \text{m} \times 5$ analogs (m ensemble members, 5 best analogs each). Significance at each grid point is assessed via bootstrap (1,000 resamples of m analogs from the $\text{m} \times 5$ pool), and confidence intervals are derived from the resampled mean differences

Figure 3 shows the changes in the multimodel multimember mean of precipitation (Fig. 3a, d, g, j, m), near-surface temperature (Fig. 3b, e, h, k, n) and SPEI12 (Fig. 3f, i, l, o) across the FP, NP, NT, and FF periods. This allows us to assess the impact of ACC on the three main variables related to drought during flow analogs. It is evident that ACC has significantly influenced drought conditions during these analogs. Firstly, near-surface temperatures are noticeably higher - up to 2 K over the continental land - relative to PI, with even higher temperature increase - between 4 and 8 K - projected for the FF period. The warming

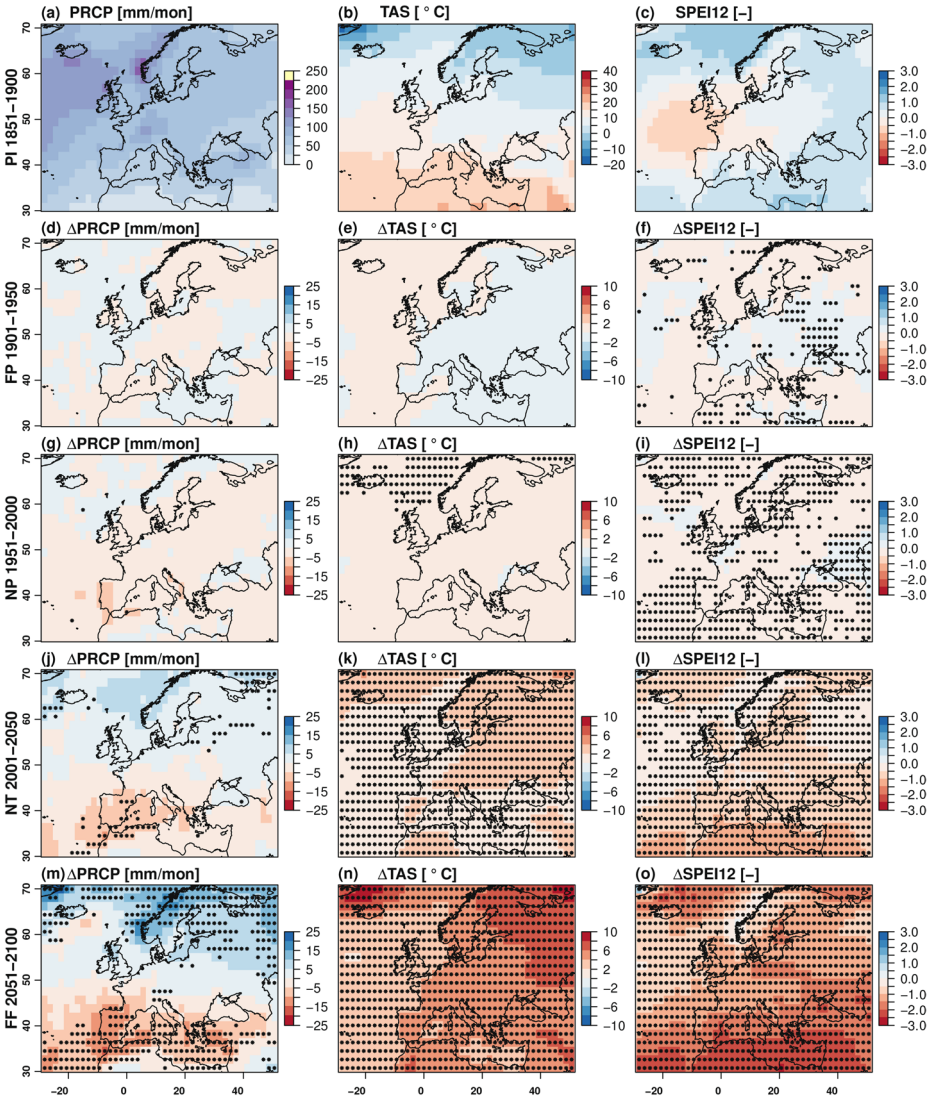

Fig. 3 Impact of ACC on drought characteristics during flow analogs. Mean (**a**) Precipitation, (**b**) Near-surface temperature, and (**c**) SPEI12 during the PI period; changes in mean (**d**) Precipitation, (**e**) Near-surface temperature, and (**f**) SPEI12 in FP relative to PI. Panels (g–i), (j–l) and (m–o) show the same quantities as (d–f), but for the NP, NT and FF periods, respectively. Years 2015–2100 follow the SSP3-7.0 scenario. Stippling indicates inter-model agreement (see Fig. 2 for details)

is particularly pronounced in northeastern Europe and Russia (Fig. 3k, n), concentrated in areas where Z500 experiences the most considerable increases during the analogs (Fig. 2m). Regarding precipitation, ACC leads to the emergence of a dry-wet south-north dipole during NT and FF periods of the analogs (Fig. 3j, m). This pattern of precipitation response is observed in most GCMs e.g., 1 and it is consistent with the poleward shift of the storm track (e.g., Harvey et al. 2020), shifts in upper tropospheric stationary waves and reduced land–water warming contrast over the Mediterranean basin (Tuel and Eltahir 2020, 2021). Interestingly, the models that agree on the Z500 anomaly response (CanESM, MIROC, and MPI) also tend to show a more marked north-south precipitation response, while the others (ACCESS, GISS, IPSL, and UKMO) tend to show a much weaker precipitation response (not shown). However, it is not straightforward to mechanistically link this to the mean Z500 or Z500 anomaly response discussed earlier.

The combined effects of changes in near-surface temperature and precipitation on drought conditions during flow analogs are reflected in the SPEI12 anomalies shown in Fig. 3l,o. The SMILES analyzed in this study confirm the significant role of ACC in making such flow analogs more prone to drought conditions, with SPEI12 substantially and significantly negative in the factual climate (NT, Fig. 3l). This trend is exacerbated even further in the FF period (Fig. 3o) under higher levels of global warming. Notably, SPEI12 anomalies during FP and NP are negligible and mostly not significant. This indicates that drought conditions would have not been worsened by ACC had such a flow analog occurred in the period from 1900 to 2000. In other words, the findings show that the same low-frequency atmospheric circulation pattern associated with the 2022 drought would have been unlikely to produce such severe impacts in the early or mid-twentieth century. Today, however, and increasingly in the future, this type of circulation leads to much more intense drought conditions—especially in the Mediterranean—due to the amplifying effects of anthropogenic climate change (ACC): not only reduced precipitation and increased evaporative demand driven by higher temperatures, but also generally higher geopotential heights that intensify atmospheric stability and dryness.

Very similar patterns to those shown in Figs. 2 and 3 are obtained when each GCM is first averaged across its ensemble members and all GCMs are then given equal weight in the multi-model mean (not shown), thus confirming that differences in ensemble size do not affect the results.

3.2 Impact of ACC on flow analogs' frequency

We next move to examine $P(\mathcal{C})$, i.e., the probability of occurrence of the flow analog associated with the 2022 drought event (see the methodology described in Sect. 2.4.1). In Fig. 4 we show the basic statistics of the number of atmospheric flow analogs for each time period (PI, FP, NP, NT, FF), across all SMILEs. We note a very large spread across ensemble members, for each time period, in the number of flow analogs, as a consequence of internal climate variability. Indeed, for each SMILE, the members of the large ensemble can exhibit a considerable range in the number of analogs - ranging from as few as a couple to as many as a few tens - during each 50-year period, highlighting the critical role of internal climate variability. In spite of this very large spread, it is evident that the number of low-frequency analogs is not substantially impacted by ACC, even in the FF period when substantial global warming is expected under the two high-end CMIP6 scenarios (SSP3-7.0 and SSP5-8.5). To

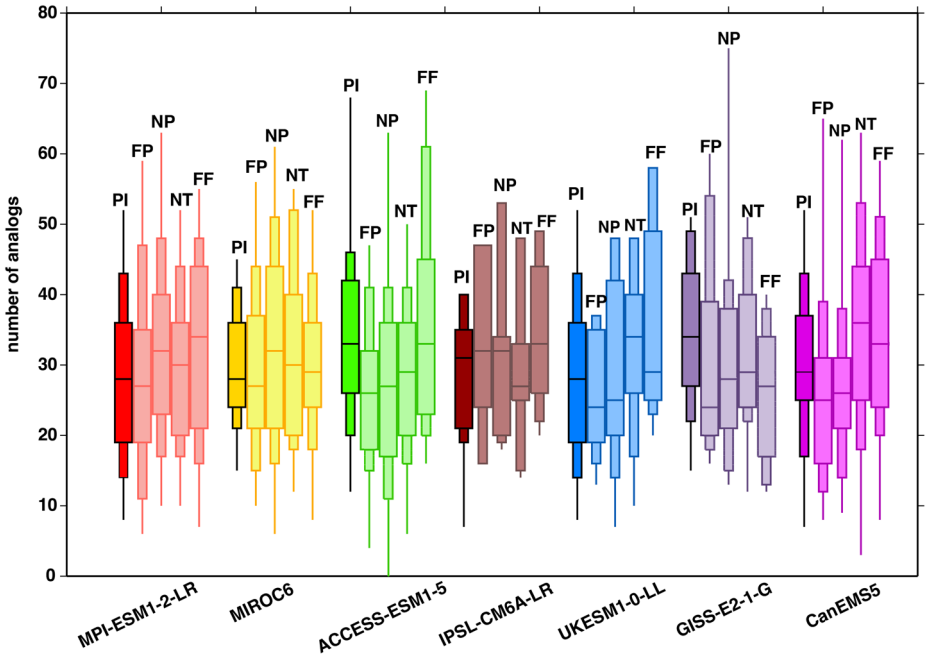

Fig. 4 Number of flow analogs under ACC. Box and whisker plots show, for each SMILE and during each time period (PI, FP, NP, NT, FF), the basic statistics in the occurrence of flow analogs: minimum, 10th percentile, 25th percentile, median, 75th percentile, 90th percentile and maximum. The box and whisker for the PI period is highlighted to better allow for comparison. NT and FF are based on SSP3-7.0 projections

more rigorously support this statement, we assess differences between periods (PI vs FP, NP, NT, and FF) for each SMILE using a parametric bootstrap approach for overdispersed count data. A Negative Binomial bootstrap is applied to generate synthetic samples that capture the extra variability, and for each replicate we compute the difference in mean counts to construct the null distribution (Hilbe 2011). The two-sided *p*-value is obtained from the proportion of bootstrap realizations exceeding the observed difference. The results show that the probability that PI and FP, NP, NT, and FF counts are drawn from the same distribution is generally larger than 5%, indicating that ACC does not significantly affect the number of analogs. Similar results are obtained for the SSP5-8.5 scenario (not shown). The insensitivity of the occurrence frequency of these flow analogs to ACC aligns with the findings of Faranda et al. (2022), based on the 20CR reanalysis for 1836–2021.

Despite the numbers of flow analogs being unaffected by ACC, drought conditions in Europe are becoming increasingly widespread during such analogs (Fig. 5). The range of the fraction (in %) of European land area affected by drought condition – that is, featuring SPEI12<-1 – during flow analogs has expanded from approximately 0–15% in the PI, FP, NP periods to around 15–30% in the NT. This indicates that the impact of ACC has become evident only in the twenty-first century. Under a low-frequency atmospheric circulation anomaly as that observed in September 2021-August 2022, the areal extent of drought over Europe would have been smaller in the twentieth century and identical to that of the counterfactual climate (PI). The impact of ACC on drought extent during flow analogs is projected

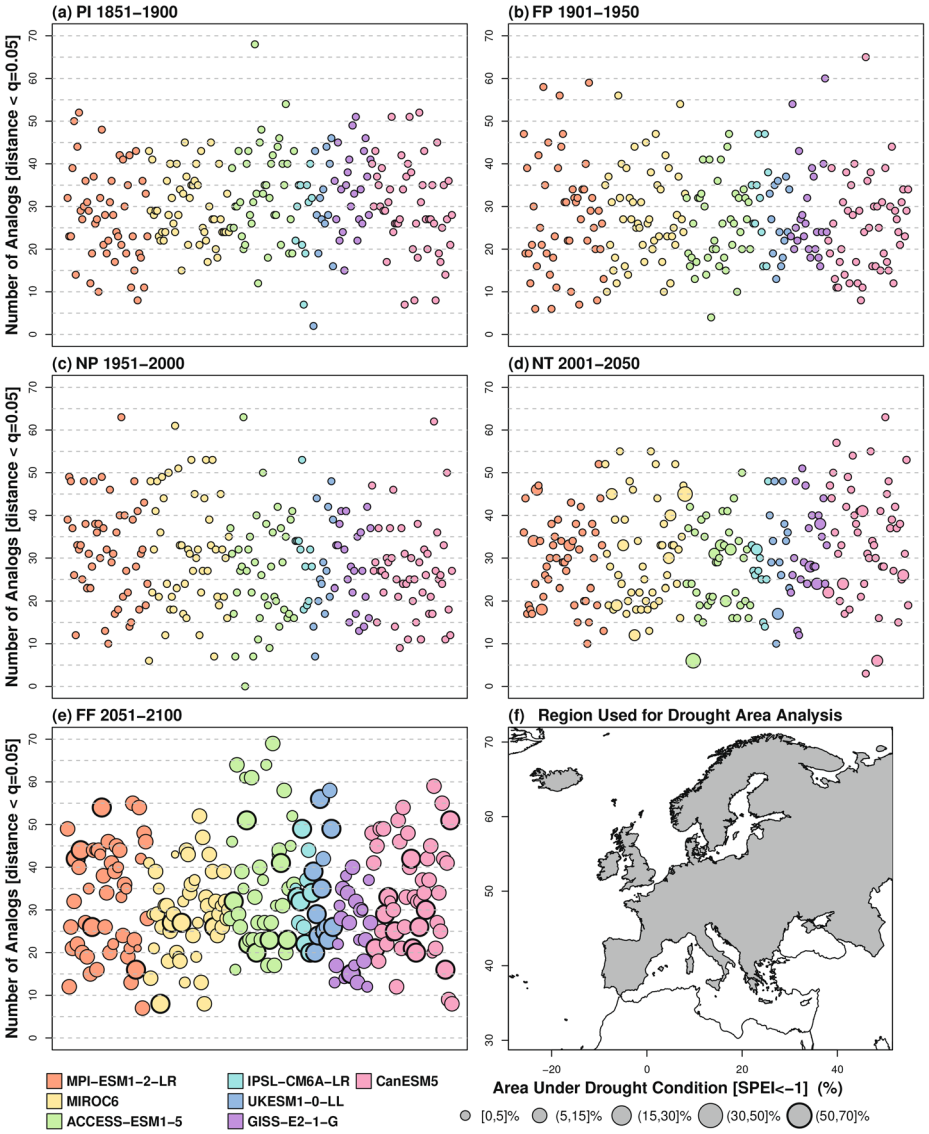

Fig. 5 The European area (percentage of grid points) under drought conditions (SPEI<-1) and the number of similar analogs (Euclidean distance less than the 0.05 quantile value) under the SSP3-7.0 scenario, across various historical and future periods: (**a**) The Pre-Industrial period (PI: 1851–1900), (**b**) The far past period (FP: 1901–1950), (**c**) The near-present period (NP: 1951–2000), (**d**) The near term period (NT: 2001–2050), and (**e**) The far future period(FF: 2051–2100); the European area considered for this analysis (**f**) Circle area is proportional to of Europe affected by drought

to substantially increase in the second part of this century under both the SSP3-7.0 and SSP5-8.5 scenario (Supplementary Fig. 11). In fact, in the FF period SMILEs indicate that 30–70% of European land area will be affected by drought conditions as flow analogs occur.

3.3 Impact of ACC on drought variability during flow analogs

Another important aspect of the effect of ACC on the 2022 European drought is the variability within the set of analogs. In other terms, how does ACC influence the diversity of drought conditions under the same flow conditions? Indeed, the occurrence of a flow analog does not lead to droughts of the same severity over Europe, as minor variations between analogs as well as smaller-scale factors, such as local boundary conditions and circulation patterns, may lead to different meteorological outcomes. It has been already shown in Sect. 3.1 (Fig. 3) that, for NT and FF, the mean values of SPEI12 during analogs tend toward more negative values over Europe, i.e., the conditional probability $P(SPEI12 < -1|\mathcal{C})$ shifts toward more negative SPEI12 values. It is interesting to explore what ACC implies regarding the variability of $P(SPEI12 < -1|\mathcal{C})$ around these more negative values. Figures 6l,o show the standard deviation of the SPEI12 values within the analog pool for each SMILE. It can be noted that, over a large part of Europe, especially in southern Europe, the spread of SPEI12 get considerably smaller as we move from FP to FF, that is, the standard deviation of $P(SPEI12 < -1|\mathcal{C})$ becomes substantially smaller as it shifts to more negative values. Consequently, both in the near term (in NT) and even more in the far future (in FF), we can expect less variability around more severe drought conditions during flow analogs. Conversely, in northern Europe (i.e., Scandinavia and western Russia), we observe an increase in the standard deviation of $P(SPEI12 < -1|\mathcal{C})$ despite an overall shift toward lower values (Fig. 6l, o). This suggests greater variability in drought conditions during flow analogs in a region that was only marginally affected by drought in 2022 (Fig. 1f). The contrasting behavior relative to southern Europe is likely attributable to the opposing precipitation response observed in this area (Fig. 3j, m). Specifically, increased precipitation in some analogs may largely offset the enhanced evaporative demand associated with a warmer climate.

4 Discussion

The wide range of climate simulations analysed in this study shows that atmospheric conditions similar to those observed during the 2022 drought, which would have been unlikely to produce severe drought impacts in the early or mid-twentieth century, now—and increasingly in the future—lead to much more pronounced drying. While the spatial pattern and frequency of the low-frequency flow analogs leading to the 2022 drought remain largely unchanged under ACC, the associated impacts are amplified. This amplification is primarily driven by thermodynamic factors, including higher temperatures, increased evaporative demand, reduced precipitation, and generally elevated geopotential heights, particularly over the Mediterranean region.

Specifically, our analysis reveals that the 12-month averaged Z500 flow analogs exhibit shape changes influenced by ACC (see Fig.2j,m). This can be attributed to ACC-induced shifts in the Z500 background state during the analog periods, resulting in enhanced ridging over eastern Europe and the Mediterranean area. The west-east differential response in Z500 may reflect either an amplified land-sea thermal contrast or a complex dynamical adjustment of the large-scale circulation to ACC, potentially involving mechanisms such as stationary Rossby waves triggered by altered land-sea thermal gradients (e.g., Tuel and

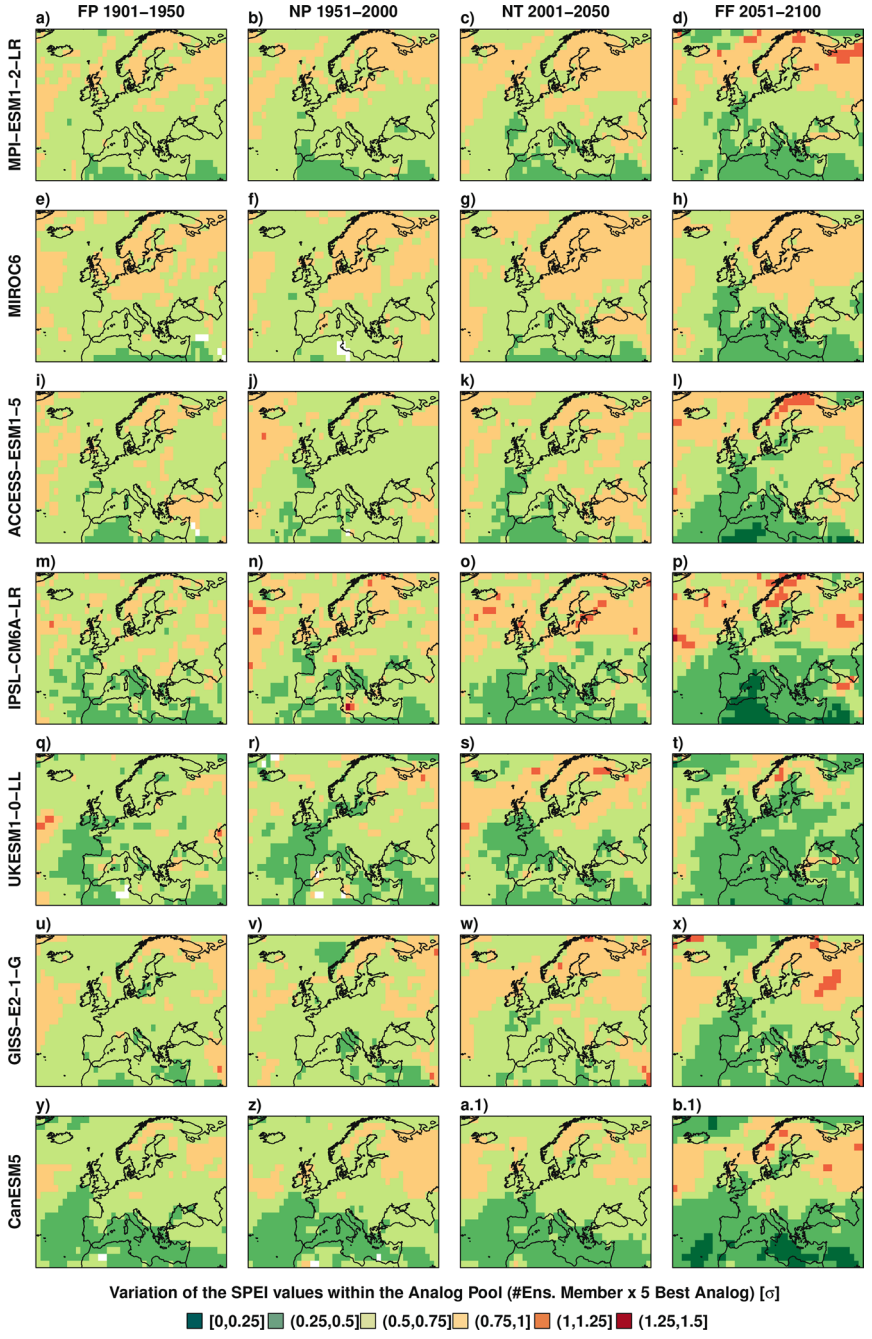

Fig. 6 Standard deviation of SPEI12 values within the analog pool obtained in the twentieth century (FP: 1901–1950, NP: 1951–2000) and twenty-first century (NT: 2001–2050, FF: 2051–2100) for each SMILE: (**a-d**) MPI-ESM1-2-LR, (**e-h**) MIROC6, (**i-l**) ACCESS-ESM1-5, (**m-p**) IPSL-CM6A-LR, (**q-t**) UKESM1-0-LL, (**u-x**) GISS-E2-1-G, (y-b.1) CanESM5. The standard deviation is evaluated considering, for each SMILE and for each period, $N = m \times 5$ analogs, with m number of ensemble members and 5 the number of best analogs found for each ensemble member

Eltahir 2020, 2021; He et al. 2023; Tahvonen et al. 2025) or modifications in teleconnection patterns (e.g., Liu et al. 2025). Climate models project greater near-surface warming over northern Eurasia compared to the adjacent Atlantic Ocean (Fig. 3k, n), providing a thermodynamic explanation for the larger tropospheric temperature increases observed over northeastern Europe. Flow analog Z500 anomalies relative to the background state display only modest and probably irrelevant changes associated with ACC (Fig. 2l, o) with large inter-model differences (Supplementary Figs. 3–9). The magnitude of these Z500 anomaly changes in the forced-future (FF) period is comparable to anomalies in other periods where ACC impact is negligible (e.g., forced-present, FP). This suggests that substantial internal decadal to multidecadal variability and inter-model differences likely obscure a clear forced signal in Z500 anomalies during the analogs.

The expansion of drought-affected areas across Europe during flow analogs (Fig. 5) is primarily driven by near-surface warming, which intensifies thermodynamic processes that increase evapotranspiration. Notably, in northeastern Europe, SPEI12 anomalies during both the NT and FF scenarios remain negative despite positive precipitation anomalies (Fig. 3m, n, o). This thermodynamic amplification of droughts has been documented in numerous recent studies (Dai 2013; Vicente-Serrano et al. 2014; Herrera et al. 2018; Ionita and Nagavciuc 2021; Gebrechorkos et al. 2025) and is considered one of the most robust impacts of ACC on meteorological extremes. In the context of the 2022 drought, we demonstrate that ACC substantially increased the affected area, producing one of the most extensive droughts recorded in Europe, with nearly 100% of the national territory impacted in some countries, such as Italy (Pascale and Ragone 2025). Furthermore, the frequency of flow analogs is projected to remain relatively stable and largely unaffected by ACC through the FF period under both high-emission scenarios (SSP3-7.0 and SSP5-8.5), as discussed in Sect. 3.2. These results suggest that atmospheric circulation dynamics will play a diminishing role in the occurrence of widespread severe droughts like that of 2022, whereas thermodynamic effects from global warming—particularly increased potential evapotranspiration—will become the dominant driver.

While we rely on a suite of large ensemble simulations from multiple General Circulation Models (GCMs) to separate the externally forced response from internal climate variability, and employ a flow-analog approach to isolate the low-frequency circulation patterns associated with the 2022 drought, certain caveats remain. First, although our analysis shows that the large-scale atmospheric low-frequency pattern linked to the 2021–2022 drought does not exhibit substantial changes under anthropogenic climate change (ACC)—neither in the present-day climate (2001–2050) nor under future projections (2051–2100)—this result must be interpreted in light of known limitations of GCMs in representing atmospheric dynamics. Previous work has highlighted persistent model biases and uncertainties in simulating circulation features, including the jet stream, blocking, and wave breaking processes (e.g., Shepherd 2014; Vautard et al. 2023; Shaw et al. 2024). These limitations affect the confidence with which one can assess changes in circulation-related drought drivers. Second, while our approach robustly assesses the frequency of analog patterns across multiple models, we do not draw strong conclusions regarding potential changes in the structure or shape of these analogs. Subtle shifts in the spatial configuration of circulation patterns—beyond frequency alone—could also influence drought severity but are more difficult to quantify and may be obscured by internal variability and model resolution constraints.

Finally, our findings reinforce the importance of using large climate model ensembles when investigating trends in low-frequency flow patterns. Internal climate variability exerts a strong influence on the occurrence of such analogs, and single or small ensembles may lead to misleading conclusions about trends or extremes (Deser 2020). Continued efforts to improve the representation of atmospheric dynamics in models, and to better constrain uncertainty through coordinated multi-model large ensemble frameworks, remain essential.

5 Conclusions

The 2022 European drought - characterized by its exceptional intensity and prolonged duration (Toreti et al. 2022b; Garrido-Perez et al. 2024; Pascale and Ragone 2025) - highlights the significant challenges posed by extreme weather events such as droughts in the context of a changing climate. Although it is well established that climate change exacerbates drought impacts by increasing temperatures and thereby enhancing evaporative demand (Dai 2013; Vicente-Serrano et al. 2014; Herrera et al. 2018; Ionita and Nagavciuc 2021; Gebrechorkos et al. 2025), the role of atmospheric circulation patterns - which modulate weather systems and low-frequency atmospheric variability - is more challenging to quantify and has only been thoroughly investigated for a few drought events to date (Harrington et al. 2016; Odoulami et al. 2023).

Our results reveal no significant change in the frequency of low-frequency flow analogs associated with the 2022 drought event, and provide inconclusive evidence regarding shifts in their spatial patterns. However, the findings suggest that the impacts of these analogs on drought severity are likely to intensify under rising temperature conditions This is accompanied by a notable reduction in the variability of the 12-month Standardized Precipitation Evapotranspiration Index (SPEI12) within the analog pool, particularly across southern Europe. These findings imply that while the role of atmospheric dynamics in driving widespread severe droughts like the 2022 event may not increase, thermodynamic effects linked to global warming—primarily through enhanced potential evapotranspiration—will increasingly dominate drought development.

We acknowledge that the methodological framework adopted in this study entails certain simplifications. As described in Sect. 2, our analysis is based on SPEI12 and on the identification of flow analogs derived from low-frequency atmospheric circulation anomalies (i.e., 12-month mean anomalies). While this approach is well suited to investigating the large-scale, persistent circulation features associated with multi-year drought conditions (e.g., Faranda et al. 2023; Pascale and Ragone 2025), it does not resolve the full dynamical complexity of drought events. In particular, it does not capture drought variability at finer temporal scales (e.g., monthly or seasonal) or the contribution of synoptic-scale atmospheric processes, nor does it explicitly account for potential land–atmosphere feedbacks, which may further amplify and sustain drought conditions (Seneviratne et al. 2021; Yoon et al. 2026). Future work employing complementary attribution approaches - such as machine learning methods (e.g., Self-Organizing Maps; Odoulami et al. 2023), storyline approaches (e.g., Shepherd 2016; Feser and Shepherd 2025), or rare event algorithms specifically designed to investigate time-persistent extreme events (e.g., Ragone and Bouchet 2021) - would be valuable to further extend and refine the present findings.

Finally, future research might extend the scope of this study, which remained focused on the major 2022 European drought event, and apply this analysis to other significant droughts occurred in the last decades in Europe (e.g., García-Herrera et al. 2007, 2019; Spinoni et al. 2015; Ionita et al. 2017; Van der Wiel et al. 2019; Moravec et al. 2021; Pascale and Ragone 2025) or in other world regions (e.g., Herrera et al. 2018; Pascale et al. 2020, 2021; Cook et al. 2022) to have a more comprehensive understanding of drought variability and climate change impacts.

Supplementary Information The online version contains supplementary material available at https://doi.org/10.1007/s10584-026-04235-z.

Acknowledgment The authors are grateful to two anonymous reviewers and the Deputy Associate Editor for their helpful comments on the first version of the manuscript. D. F. received support from the European Unions Horizon 2020 research and innovation programme under grant agreement No. 101003469(XAIDA) and the Marie Sklodowska-Curie grant agreement No. 956396 (EDIPI).

Author contributions Burak Bulut: Data curation; Formal Analysis; Visualization; Writing: Review & Editing. Salvatore Pascale: Conceptualization; Writing: Original Draft Preparation; Review & Editing. Davide Faranda: Conceptualization; Writing: Review & Editing.

Data availability ECMWF Reanalysis v5 (ERA5) data used in this study are available at Hersbach et al. (2020). The SPEIbase data are avialble at https://spei.csic.es/database.html. The CRU TS 4.08 precipitation dataset is available online at https://data.ceda.ac.uk/badc/cru/data/cru_ts/cru_ts_4.08. SMILEs have been downloaded from the CMIP6 archive at https://esgf-node.llnl.gov/search/cmip6/.

Declarations

Ethical approval Not applicable.

Permission to reproduce material from other sources Not applicable.

Competing interests The authors declare no competing interests nor conflicts of interest.

References

Allan RP, Hawkins E, Bellouin N, Collins B (2021) IPCC, 2021: Summary for Policymakers. Clim Change 2021: Phys Sci Basis. Contribution Work Group I to Sixth Assess Report the Intergovernmental Panel Clim Change. 3–32

Anderson TG, McKinnon KA, Pons D, Anchukaitis KJ (2023) How exceptional was the 2015–2019 central American drought? Geophys Res Lett 50(21):e2023GL105391. https://doi.org/10.1029/2023GL105391

Bakke SJ, Ionita M, Tallaksen LM (2023) Recent European drying and its link to prevailing large-scale atmospheric patterns. Sci Rep 13(1):21921. https://doi.org/10.1038/s41598-023-48861-4

Barnston AG, Livezey RE (1987) Classification, seasonality and persistence of low-frequency atmospheric circulation patterns. Mon Wea Rev 115(6):1083–1126. https://doi.org/10.1175/1520-0493(1987)115%3C1083:CSAPOL%3E2.0.CO;2

Baruth B, Bassu S, W. B, Biavetti I, Bratu M, Cerrani I, Chemin Y, Claverie M, De Palma P, Fumagalli D, Manfron G, Morel J, Nisini L, Panarello L, Ronchetti G, Seguini L, Tarnavsky E, van den Berg M, Zajac Z, Zucchini A (2022) Crop monitoring in Europe, June 2022. JRC MARS Bull 30

Beguería S, Vicente-Serrano SM, Reig F, Latorre B (2014) Standardized precipitation evapotranspiration index (SPEI) revisited: parameter fitting, evapotranspiration models, tools, datasets and drought monitoring. Int J Climatol 34(10):3001–3023. https://doi.org/10.1002/joc.3887

Bevacqua E, Rakovec O, Schumacher DL, Kumar R, Thober S, Samaniego L, Seneviratne SI, Zscheischler J (2024) Direct and lagged climate change effects intensified the 2022 European drought. Nat Geosci 17(11):1100–1107. https://doi.org/10.1038/s41561-024-01559-2

Brönnimann S (2007) Impact of El Niño–Southern Oscillation on European climate. Rev Geophysics 45(3):RG3003. https://doi.org/10.1029/2006RG000199
Christidis N, Stott PA (2015) Changes in the geopotential height at 500 hpa under the influence of external climatic forcings. Geophys Res Lett 42(24): 10798–10806. https://doi.org/10.1002/2015GL066669
Clifford C (2022) Italy has declared a state of emergency because of drought: there is no doubt that climate change is having an effect, the prime minister said. https://www.cnbc.com/2022/07/05/italy-declared-a-state-of-emergency-because-of-drought-in-the-po-river.html
Compo GP, Whitaker JS, Sardeshmukh PD, Matsui N, Allan RJ, Yin X, Gleason BE, Vose RS, Rutledge G, Bessemoulin P, Brönnimann S, Brunet M, Crouthamel RI, Grant AN, Groisman PY, Jones PD, Kruk MC, Kruger AC, Marshall GJ, Maugeri M, Mok HY, Nordli Ø, Ross TF, Trigo RM, Wang XL, Woodruff SD, Worley SJ (2011) The twentieth century reanalysis project. Quart J R Meteoro Soc 137(654):1–28. https://doi.org/10.1002/qj.776
Cook BI, Smerdon JE, Cook ER, Williams AP, Anchukaitis KJ, Mankin JS, Allen K, Andreu-Hayles L, Ault TR, Belmecheri S, Coats S, Coulthard B, Fosu B, Grierson P, Griffin D, Herrera DA, Ionita M, Lehner F, Leland C, Marvel K, Morales MS, Mishra V, Ngoma J, Nguyen HTT, O'Donnell A, Palmer J, Rao MP, Rodriguez-Caton M, Seager R, Stahle DW, Stevenson S, Thapa UK, Varuolo-Clarke AM, Wise EK (2022) Megadroughts in the common era and the anthropocene. Nat Rev Earth Environ 3(11):741–757. https://doi.org/10.1038/s43017-022-00329-1
Dai A (2013) Increasing drought under global warming in observations and models. Nat Clim Change 3(1):52. https://doi.org/10.1038/nclimate1633
Deser C (2020) Certain uncertainty: the role of internal climate variability in projections of regional climate change and risk management. Earth's Future 8(12):e2020EF001854. https://doi.org/10.1029/2020EF001854
Deser C, Lehner F, Rodgers KB, Ault T, Delworth TL, DiNezio PN, Fiore A, Frankignoul C, Fyfe JC, Horton DE (2020) Insights from earth system model initial-condition large ensembles and future prospects. In: Nature climate change. Nature Publishing Group, Publisher, pp 1–10. ISBN: 1758-6798
Doane-Solomon R, Woollings T, Simpson IR (2025) Dynamic contributions to recent observed wintertime precipitation trends in Mediterranean-type climate regions. Geophys Res Lett 52(12):e2024GL114258. https://doi.org/10.1029/2024GL114258
Eyring V, Bony S, Meehl GA, Senior CA, Stevens B, Stouffer RJ, Taylor KE (2016) Overview of the coupled model intercomparison project phase 6 (CMIP6) experimental design and organization. Geosci Model Dev 9(5):1937–1958. https://doi.org/10.5194/gmd-9-1937-2016
Faranda D, Bourdin S, Ginesta M, Krouma M, Noyelle R, Pons F, Yiou P, Messori G (2022) A climate-change attribution retrospective of some impactful weather extremes of 2021. Weather Clim Dynam 3(4):1311–1340. https://doi.org/10.5194/wcd-3-1311-2022
Faranda D, Pascale S, Bulut B (2023) Persistent anticyclonic conditions and climate change exacerbated the exceptional 2022 European-Mediterranean drought. Env Res Lett 18:034030
Feser F, Shepherd T (2025) The concept of spectrally nudged storylines for extreme event attribution. Commun Earth Environ 6(1):1–8. https://doi.org/10.1038/s43247-025-02659-6
García-Herrera R, Garrido-Perez JM, Barriopedro D, Ordóñez C, Vicente-Serrano SM, Nieto R, Gimeno L, Sorí R, Yiou P (2019) The European 2016/17 drought. J Climate 32(11):3169–3187. https://doi.org/10.1175/JCLI-D-18-0331.1
García-Herrera R, Hernández A, Barriopedro D, Trigo R, Trigo I, Mendes M (2007) The outstanding 2004/05 drought in the Iberian Peninsula: associated atmospheric circulation. J Hydrometeorol 8(3):483–498. https://doi.org/10.1175/JHM578.1
Garrido-Perez JM, Vicente-Serrano SM, Barriopedro D, García-Herrera R, Trigo R, Beguería S (2024) Examining the outstanding Euro-Mediterranean drought of 2021–2022 and its historical context. J Hydrol 630:130653. https://doi.org/10.1016/j.jhydrol.2024.130653
Gastineau G, Frankignoul C (2015) Influence of the North Atlantic ocean on the decadal variability of the North Atlantic Oscillation. J Climate 28(19):7659–7677. https://doi.org/10.1175/JCLI-D-15-0007.1
Gebrechorkos SH, Sheffield J, Vicente-Serrano SM, Funk C, Miralles DG, Peng J, Dyer E, Talib J, Beck HE, Singer MB, Dadson SJ (2025) Warming accelerates global drought severity. Nature 642(8068):628–635. https://doi.org/10.1038/s41586-025-09047-2
Harrington LJ, Gibson PB, Dean SM, Mitchell D, Rosier SM, Frame DJ (2016) Investigating event-specific drought attribution using self-organizing maps. J Geophys Res Atmos 121(21):12766–12780 https://doi.org/10.1002/2016JD025602
Harris I, Osborn TJ, Jones P, Lister D (2020) Version 4 of the CRU TS monthly high-resolution gridded multivariate climate dataset. Sci DataSci Data 7(1):1–18. https://doi.org/10.1038/s41597-020-0453-3
Harvey BJ, Cook P, Shaffrey LC, Schiemann R (2020) The response of the northern hemisphere storm tracks and jet streams to climate change in the CMIP3, CMIP5, and CMIP6 climate models. JGR Atmospheres 125(23):e32701. https://doi.org/10.1029/2020JD032701

He Y, Zhu X, Sheng Z, He M (2023) Resonant waves play an important role in the increasing heat waves in northern hemisphere mid-latitudes under global warming. Geophys Res Lett 50(14):e2023GL104839. https://doi.org/10.1029/2023GL104839

Herrera DA, Ault TR, Fasullo JT, Coats SJ, Carrillo CM, Cook BI, Williams AP (2018) Exacerbation of the 2013–2016 Pan-Caribbean drought by anthropogenic warming. Geophys Res Lett 45(19):,10,619–,10,626. https://doi.org/10.1029/2018GL079408

Hersbach H, Bell B, Berrisford P, Hirahara S, Horányi A, Muñoz-Sabater J, Nicolas J, Peubey C, Radu R, Schepers D, Simmons A, Soci C, Abdalla S, Abellan X, Balsamo G, Bechtold P, Biavati G, Bidlot J, Bonavita M, De Chiara G, Dahlgren P, Dee D, Diamantakis M, Dragani R, Flemming J, Forbes R, Fuentes M, Geer A, Haimberger L, Healy S, Hogan RJ, Hólm E, Janisková M, Keeley S, Laloyaux P, Lopez P, Lupu C, Radnoti G, de Rosnay P, Rozum I et al (2020) The ERA5 global reanalysis. Quart J R Meteoro Soc 146(730):1999–2049. https://doi.org/10.1002/qj.3803

Hilbe JM (2011) Negative binomial regression, 2 edn. Cambridge University Press

Hurrell J (1995) Decadal trends in the North Atlantic Oscillation: regional temperatures and precipitation. Science 269(5224):676–679. https://doi.org/10.1126/science.269.5224.676

Ionita M, Nagavciuc V (2021) Changes in drought features at the European level over the last 120 years. Nat Hazards Earth Syst Sci 21(5):1685–1701. https://doi.org/10.5194/nhess-21-1685-2021

Ionita M, Tallaksen LM, Kingston DG, Stagge JH, Laaha G, Van Lanen AJ, Scholz P, Chelcea SM, Haslinger K (2017) The European 2015 drought from a climatological perspective. Hydrol Earth Syst Sci 21(3):1397–1419. https://doi.org/10.5194/hess-21-1397-2017

Jézéquel A, Cattiaux J, Naveau P, Radanovics S, Ribes A, Vautard R, Vrac M, Yiou P (2018) Trends of atmospheric circulation during singular hot days in Europe. Environ Res Lett 13(5):054007. https://doi.org/10.1088/1748-9326/aab5da

Jézéquel A, Yiou P, Radanovics S, Vautard R (2018) Analysis of the exceptionally warm December 2015 in France using flow analogues. Bull Am Meteorolog Soc 99(1):S76–S79. https://doi.org/10.1175/BAMS-D-17-0103.1

Kay JE et al (2015) The community Earth System model (CESM) large ensemble project: a community resource for studying climate change in the presence of internal climate variability. Bull Am Meteorolog Soc 96(8):1333–1349. https://doi.org/10.1175/BAMS-D-13-00255.1

Keeley SPE, Sutton RT, Shaffrey LC (2012) The impact of North Atlantic sea surface temperature errors on the simulation of the North Atlantic Oscillation. Clim Dyn 39:1673–1693

Kingston DG, Stagge JH, Tallaksen LM, Hannah DM (2015) European-scale drought: understanding connections between atmospheric circulation and meteorological drought indices. J Climate 28(2):505–516. https://doi.org/10.1175/JCLI-D-14-00001.1

Knight JR, Allan RJ, Folland CK, Vellinga M, Mann ME (2005) A signature of persistent natural thermohaline circulation cycles in observed climate. Geophys Res Lett 32(20):L20708. https://doi.org/10.1029/2005GL024233

Kreibich H, Van Loon AF, Schröter K, Ward PJ, Mazzoleni M, Sairam N, Abeshu GW, Agafonova S, AghaKouchak A, Aksoy H, Alvarez-Garreton C, Aznar B, Balkhi L, Barendrecht MH, Biancamaria S, Bos-Burgering L, Bradley C, Budiyono Y, Buytaert W, Capewell L, Carlson H, Cavus Y, Couasnon A, Coxon G, Daliakopoulos I, de Ruiter MC, Delus C, Erfurt M, Esposito G, François D, Frappart F, Freer J, Frolova N, Gain AK, Grillakis M, Grima JO, Guzmán DA, Huning LS, Ionita M, Kharlamov M et al (2022) The challenge of unprecedented floods and droughts in risk management. Nature 608(7921):80–86. https://doi.org/10.1038/s41586-022-04917-5

Kucharski F, Molteni F, Bracco A (2006) Decadal interactions between the western tropical Pacific and the north Atlantic oscillation. Clim Dyn 26(1):79–91. https://doi.org/10.1007/s00382-005-0085-5

Lehner F, Coats S, Stocker TF, Pendergrass AG, Sanderson BM, Raible CC, Smerdon JE (2017) Projected drought risk in 1.5°C and 2°C warmer climates. Geophys Res Lett 44:7419–7428

Lehner F, Deser C (2023) Origin, importance, and predictive limits of internal climate variability. Environ Res.: Clim 2(2):023001. https://doi.org/10.1088/2752-5295/accf30

Liu Q, B. J, Jungclaus JH, Matei D (2025) More extreme summertime North Atlantic Oscillation under climate change. Commun Earth Environ 6(1):474. https://doi.org/10.1038/s43247-025-02422-x

Maher N, Milinski S, Ludwig R (2021) Large ensemble climate model simulations: introduction, overview, and future prospects for utilising multiple types of large ensemble. Earth Syst Dynam 12(2):401–418. https://doi.org/10.5194/esd-12-401-2021

Massari C, Avanzi F, Bruno G, Gabellani S, Penna D, Camici S (2022) Evaporation enhancement drives the European water-budget deficit during multi-year droughts. Hydrol Earth Syst Sci 26(6):1527–1543. https://doi.org/10.5194/hess-26-1527-2022

McKee T, Doesken N, Kleist J (1993) The relationship of drought frequency and duration to time scales. In Proceedings of the 8th Conference on Applied Climatology, American Meteorological Society, Anaheim, CA. Boston, MA. 17–22 January 1993

Milinski S, N. M, Olonscheck D (2020) How large does a large ensemble need to be? Earth Syst Dynam 11(4):885–901. https://doi.org/10.5194/esd-11-885-2020

Montanari A, Nguyen H, Rubinetti S, Ceola S, Galelli S, Rubino A, Zanchettin D (2023) Why the 2022 Po river drought is the worst in the past two centuries. Sci Adv 9(32):eadg8304. https://doi.org/10.1126/sciadv.adg8304

Moravec V, Markonis Y, Rakovec O, Svoboda M, Trnka M, Kumar R, Hanel M (2021) Europe under multi-year droughts: how severe was the 2014–2018 drought period? Environ Res Lett 16(3):034062. https://doi.org/10.1088/1748-9326/abe828

NAS (2016) Attribution of extreme weather events in the context of climate change. Natl Acad Sci Eng Med, 166pp. https://doi.org/10.17226/21852

Navarra L (2022) Italy's salty Po Delta hurting agriculture, fisheries. https://apnews.com/article/droughts-weather-italy-76923f07ddf081ad78d1bc41d3bd93cf

Odoulami RC, Wolski P, New M (2023) Attributing the driving mechanisms of the 2015–2017 drought in the western Cape (South Africa) using self-organising maps. Environ Res Lett 18(7):074043. https://doi.org/10.1088/1748-9326/ace26f

Otto FEL, Wolski P, Lehner F, Tebaldi C, van Oldenborgh G, Hogesteeger S, Singh R, Holden P, Fuckar N, Odoulami R, New M (2018) Anthropogenic influence on the drivers of the western Cape drought 2015–2017. Environ Res Lett 13(12):124010. https://doi.org/10.1088/1748-9326/aae9f9

Pascale S, Kapnick S, Delworth T, Hidalgo H, Cooke W (2021) Natural variability vs forced signal in the 2015–2019 central American drought. Climatic Change 168(3–4):1–21. https://doi.org/10.1007/s10584-021-03228-4

Pascale S, Kapnick S, Delworth W, Cooke TLA (2020) Increasing risk of another Cape Town "day zero" drought in the 21st century. In Proceedings of the National Academy of Sciences of the United States of America, vol 117. pp 29495–29503

Pascale S, Ragone F (2025) Widespread multi-year droughts in Italy: identification and causes of development. Intl J Climatol 45(8):e8827. https://doi.org/10.1002/joc.8827

Ragone F, Bouchet F (2021) Rare event algorithm study of extreme warm summers and heatwaves over Europe. Geophys Res Lett 48(12):e2020GL091197. https://doi.org/10.1029/2020GL091197

Riahi K, Van Vuuren DP, Kriegler E, Edmonds J, O'neill BC, Fujimori S, Bauer N, Calvin K, Dellink R, Fricko O (2017) The shared socioeconomic pathways and their energy, land use, and greenhouse gas emissions implications: an overview. Global Environ Change 42:153–168. https://doi.org/10.1016/j.gloenvcha.2016.05.009

Schumacher DL, Zachariah M, Otto F, Barnes C, Philip S, Kew S, Vahlberg M, Singh R, Heinrich D, Arrighi J, van Aalst M, Hauser M, Hirschi M, Bessenbacher V, Gudmundsson L, Beaudoing HK, Rodell M, Li S, Yang W, Vecchi GA, Harrington LJ, Lehner F, Balsamo G, Seneviratne SI (2024) Detecting the human fingerprint in the summer 2022 western–central European soil drought. Earth Syst Dynam 15(1):131–154. https://doi.org/10.5194/esd-15-131-2024

Seneviratne S, Zhang X, Adnan M, Badi W, Dereczynski C, Di Luca A, Ghosh S, Iskandar I, Kossin J, Lewis S, Otto F, Pinto I, Satoh M, Vicente-Serrano S, Wehner M, Zhou B (2021) Weather and climate extreme events in a changing climate. In: Masson-Delmotte V et al (eds) Climate change 2021: the physical science basis. Contribution of working group I to the sixth assessment report of the Intergovernmental Panel on Climate Change. Cambridge University Press, Cambridge, United Kingdom and New York, NY, USA, pp 1513–1766

Shaw TA, Arblaster JM, Birner T, Butler AH, Domeisen DIV, Garfinkel CI, Garny H, Grise KM, Karpechko AY (2024) Emerging climate change signals in atmospheric circulation. AGU Adv 5(6):e2024AV001297. https://doi.org/10.1029/2024AV001297

Shaw TA, Arias P, Collins M, Coumou D, Diedhiou A, Garfinkel C, Jain S, Roxy M, Kretschmer M, Leung L, Narsey S, Martius O, Seager R, Shepherd T, Sörensson A, Stephenson T, Taylor M, Wang L (2024) Regional climate change: consensus, discrepancies, and ways forward. Front Clim 6:1391634. https://doi.org/10.3389/fclim.2024.1391634

Shepherd TG (2014) Atmospheric circulation as a source of uncertainty in climate change projections. Nat Geosci 7(10):703. https://doi.org/10.1038/ngeo2253

Shepherd TG (2016) A common framework for approaches to extreme event attribution. Curr Clim Change Rep 2(1):28–38. https://doi.org/10.1007/s40641-016-0033-y

Shepherd TG (2019) Storyline approach to the construction of regional climate change information. Proc R Soc A 475(2225):20190013. https://doi.org/10.1098/rspa.2019.0013

Simpson IR, Shaw TA, Ceppi P, Clement AC, Fischer E, Grise KM, Pendergrass AG, Screen JA, Wills RCJ, Woollings T, Blackport R, Kang JM, Po-Chedley S (2025) Confronting earth system model trends with observations. Sci Adv 11(11):eadt8035. https://doi.org/10.1126/sciadv.adt8035

Sousa PM, Blamey RC, Reason CJC, Ramos AM, Trigo RM (2018) The 'day zero' Cape Town drought and the poleward migration of moisture corridors. Environ Res Lett 13(12):124025. https://doi.org/10.1088/1748-9326/aaebc7

Spinoni J, Naumann G, Carrao H, Barbosa P, Vogt J (2013) World drought frequency, duration, and severity for 1951-2010. Int J Climatol 34(8):2792–2804. https://doi.org/10.1002/joc.3875

Spinoni J, Naumann G, Vogt J, Barbosa P (2015) The biggest drought events in Europe from 1950 to 2012. J Hydrol Reg Stud 3:509–524. https://doi.org/10.1016/j.ejrh.2015.01.001

Staten PW, Lu J, Grise KM, Davis T, Birner SMA (2018) Re-examining tropical expansion. Nat Clim Change 8(9):768–775. https://doi.org/10.1038/s41558-018-0246-2

Sutton RT, Hodson DLR (2005) Atlantic ocean forcing of north American and European summer climate. Science 309(5731):115–118. https://doi.org/10.1126/science.1109496

Tahvonen S, Köhler D, Räisäen P, Sinclair VA (2025) Response of northern hemisphere Rossby wave breaking to changes in sea surface temperature and sea ice cover. Weather Clim Dyn 6(4):1299–1317. https://doi.org/10.5194/wcd-6-1299-2025

Teutschbein C, Albrecht F, Blicharska M, Tootoonchi F, Stenfors E, Grabs T (2023) Drought hazards and stakeholder perception: unraveling the interlinkages between drought severity, perceived impacts, preparedness, and management. Ambio 52(7):1262–1281. https://doi.org/10.1007/s13280-023-01849-w

Toreti A et al (2022a) Drought in Europe August 2022. Publications Office of the European Union, Luxembourg. https://doi.org/10.2760/781876

Toreti A et al (2022b) Drought in northern Italy. https://data.europa.eu/doi/10.2760/781876

Tuel A, Eltahir EAB (2020) Why is the Mediterranean a climate change hot spot? J Climate 33(14):5829–5843. https://doi.org/10.1175/JCLI-D-19-0910.1

Tuel A, Eltahir EAB (2021) Mechanisms of European summer drying under climate change. J Climate 34(22):8913–8931. https://doi.org/10.1175/JCLI-D-20-0968.1

Van der Wiel K, Batelaan T, Wanders N (2022) Large increases of multi-year droughts in north-western Europe in a warmer climate. Clim Dyn 60(5–6):1781–1800. https://doi.org/10.1007/s00382-022-06373-3

Van der Wiel K, Wanders N, Selten FM, Bierkens MFP (2019) Added value of large ensemble simulations for assessing extreme river discharge in a 2°C warmer world. Geophys Res Lett 46(4):2093–2102

Vautard R, Cattiaux J, Happé T, Singh J, Bonnet R, Cassou C, Coumou D, D'Andrea F, Faranda D, Fischer E, Ribes A, Sippel S, Yiou P (2023) Heat extremes in western Europe increasing faster than simulated due to atmospheric circulation trends. Nat Commun 14(1):6803. https://doi.org/10.1038/s41467-023-42143-3

Vautard R, van Oldenborg G, Bonnet R, Li S, Robin Y, Kew S, Philip S, Soubeyroux J, Dubuisson B, N V, Riechstein M, Otto F (2021) Human influence on growing period frosts like the early April 2021 in Central France. Nat Hazards Earth Syst Sci 23:1045–1058. https://nhess.copernicus.org/articles/23/1045/2023/

Vicente-Serrano S, Beguería S, I LJ (2010) A multiscalar drought index sensitive to global warming: the Standardized Precipitation Evapotranspiration Index. J Climate 23(7):1696–1718. https://doi.org/10.1175/2009JCLI2909.1

Vicente-Serrano S, López-Moreno JI, Beguería S, Lorenzo-Lacruz J, Sanchez-Lorenzo A, García-Ruiz JM, Azorin-Molina C, Morán-Tejeda E, Revuelto J, Trigo R, Coelho F, Espejo F (2014) Evidence of increasing drought severity caused by temperature rise in southern Europe. Environ Res Lett 9(4):044001. https://doi.org/10.1088/1748-9326/9/4/044001

Wendt DE, Bloomfield JP, Van Loon AF, Garcia M, Heudorfer B, Larsen J, Hannah DM (2021) Evaluating integrated water management strategies to inform hydrological drought mitigation. Nat Hazards Earth Syst Sci 21(10):3113–3139. https://doi.org/10.5194/nhess-21-3113-2021

Wolski P (2018) How severe is Cape Town's "day zero" drought? Significance 15(2):24–27. https://doi.org/10.1111/j.1740-9713.2018.01127.x

Woollings T, Franzke C, Hodson D, Dong B, Barnes EA, Raible CC, Pinto JG (2015) Contrasting interannual and multidecadal NAO variability. Clim Dyn 45(1–2):539–556. https://doi.org/10.1007/s00382-014-2237-y

Yiou P (2014) AnaWEGE: a weather generator based on analogues of atmospheric circulation. Geosci Model Dev 7(2):531–543. https://doi.org/10.5194/gmd-7-531-2014

Yiou P, Faranda D, Thao S, Vrac M (2021) Projected changes in the atmospheric dynamics of climate extremes in France. Atmosphere 12(11):1440. https://doi.org/10.3390/atmos12111440

Yiou P, Jézéquel A, Naveau P, Otto FEL, Vautard R, Vrac M (2017) A statistical framework for conditional extreme event attribution. Adv Stat Clim Meteorol Oceanogr 3(1):17–31. https://doi.org/10.5194/ascmo-3-17-2017

Yiou P, Nogaj M (2004) Extreme climatic events and weather regimes over the north Atlantic: When and where? Geophys Res Lett 31(7):1–4. https://doi.org/10.1029/2003GL019119

Yoon D, Chen J, Hsu H, Findell KL (2026) Variations in land-atmosphere coupling during drought-heatwave events. Commun Earth Environ 7(1):1–12. https://doi.org/10.1038/s43247-025-02977-9

Zampieri M, Lionello P, Scoccimarro E (2017) Atlantic Multi-decadal Oscillation influence on weather regimes over Europe and the mediterranean. Clim Dyn 48:1705–1723